Meson Production in $p+d$ Collisions and the $I=0$ π-π Interaction. II. Study of the Reactions $p+d \rightarrow He^3+\pi^0$ and $p+d \rightarrow H^3+\pi^{+*\dagger}$

NORMAN E. BOOTH‡
Lawrence Radiation Laboratory, University of California, Berkeley, California
(Received 17 June 1963)

Absolute cross sections for the reactions $p+d \rightarrow He^3+\pi^0$ and $p+d \rightarrow H^3+\pi^+$ have been measured at several angles and energies. The experimental He^3 and H^3 momentum resolution has been computed and compared with the results obtained for these two reactions. By comparing experimental data on these reactions with the reaction $p+p \rightarrow d+\pi^+$ it has been possible to compute the impulse-approximation integral relating the processes. The results are in good agreement with other experiments.

I. INTRODUCTION

MEASUREMENTS of the reactions $p+d \rightarrow He^3+\pi^0$ and $p+d \rightarrow H^3+\pi^+$ are valuable to us for several reasons:

(1) By comparing the widths and shapes of the single-pion (1π) peaks with our resolution calculations, we can compute with confidence the experimental resolutions at He^3 momenta corresponding to 2π production.

(2) By comparing our results with measurements made by other groups, we can check the reliability of our computations of absolute cross sections.

(3) Measured cross sections for these reactions combined with the cross section for $p+p \rightarrow d+\pi^+$ allow one to compute the He^3 form factor, i.e., the probability that the three nucleons in the reaction $p+d \rightarrow He^3+n\pi$ stick together to form He^3 as a function of the He^3 momentum.

(4) The knowledge of the ratio $\sigma(1\pi)/\sigma(2\pi)$ may give some information on the mechanism of the two-pion production.

(5) The ratio of the cross sections of these two reactions gives a direct test of charge independence.

II. DIFFERENTIAL CROSS SECTIONS AND CHARGE INDEPENDENCE

Differential cross sections for the reactions $p+d \rightarrow He^3+\pi^0$ and $p+d \rightarrow H^3+\pi^+$ were computed by integration under the data points of Fig. 12 of the preceding paper and Fig. 2 of Ref. 1. The results are given in Table I. Errors have not been computed in detail, the assigned errors of $\pm 10\%$ being partly statistical and partly due to uncertainties in solid angle, D_2 density, and momentum acceptance. The consistency of the cross sections from run to run leads us to believe that there are no important systematic errors, but there could be an error of 10% or more in the estimate of the ion-chamber multiplication factor upon which the absolute cross sections are based.

Charge independence predicts that the cross sections $(H^3+\pi^+)/(He^3+\pi^0)$ should be in the ratio 2:1 apart from electromagnetic corrections. The ratio we obtain at 743 MeV and $\theta_\pi^*=130°$ is $2(1.00\pm 0.05)$. The electromagnetic corrections have been estimated at lower proton energies by Köhler,[2] and are in the direction of increasing the ratio but are expected to be less than 10%. Thus, our result is consistent with charge independence. Other measurements have been made at[3] 450 MeV and[4] 591 MeV.

TABLE I. Cross sections for $p+d \rightarrow He^3+\pi^0$ and $p+d \rightarrow H^3+\pi^+$.

Reaction	Run	Incident proton energy (MeV)	Lab angle (deg)	$(d\sigma/d\Omega)_{lab}$ (μb/sr)	C. m. pion angle (deg)	$(d\sigma/d\Omega)_{c.m.}$ (μb/sr)
$He^3+\pi^0$	1	562	11.7	4.66±0.47	125.0	0.21 ±0.02
	1	624	11.7	3.19±0.32	127.5	0.16 ±0.02
	1	648	11.7	2.19±0.29	128.2	0.15 ±0.02
	1	695	11.7	1.86±0.19	129.6	0.10 ±0.01
	1	743	11.7	1.62±0.16	131.0	0.094±0.009
	2	743	11.8	1.57±1.16	130.5	0.091±0.009
$H^3+\pi^+$	2	743	11.8	6.27±0.62	24.0	1.25 ±0.13
	2	743	11.8	3.08±0.31	130.0	0.18 ±0.02
$He^3+\pi^0$	3	750	13.5	2.10±0.10	123.2	0.12 ±0.01
	3	750	15.7	2.32±0.08	111.2	0.12 ±0.01

III. MOMENTUM RESOLUTION

The determination of solid angle, target thickness, proton beam intensity and "momentum acceptance" have already been discussed in paper I. We now briefly outline the calculation of the momentum resolution. For convenience of calculation the factors affecting the momentum resolution may be split up into two parts, those which can be approximated by Gaussians and those which cannot. In the first category we have multiple scattering and angular divergence of the proton beam; in the second, energy loss in the target and finite angular definition, beam dimensions, and image and grid sizes. Two other factors that should be con-

* Work performed under the auspices of the U. S. Atomic Energy Commission.
† Paper II in a series comprising UCRL-10407, 10408, 10409, and 10410.
‡ Present address: The Enrico Fermi Institute for Nuclear Studies, University of Chicago, Chicago, Illinois.
[1] A. Abashian, N. E. Booth, and K. M. Crowe, Phys. Rev. Letters **5**, 258 (1960).
[2] H. S. Köhler, Phys. Rev. **118**, 1345 (1960).
[3] A. V. Crewe, B. Ledley, E. Lillethun, S. Marcowitz, and C. Rey, Phys. Rev. **118**, 1091 (1960).
[4] D. Harting, J. C. Kluyver, A. Kusumegi, R. Rigopoulos, A. M. Sachs, G. Tibell, G. Vanderhaegle, and G. Weber, Phys. Rev. **119**, 1716 (1960).

sidered are magnetic aberrations and energy spread of the proton beam. We took care to minimize the aberrations of the momentum-analyzing system, and since we believe them to be small, we do not include them in the resolution calculation. The energy spread of the proton beam is not well known, but we can set an upper limit on it from the geometry shown in Fig. 2 of paper I. In practice we calculate the energy spread by comparing the momentum resolution for a monoenergetic proton beam with the observed widths of the 1π production peaks.

In what follows each factor is considered separately, and all are summarized in Table II.

TABLE II. Factors affecting momentum resolution.

Gaussian factors			
	Standard deviation of Gaussian (MeV/c)		
Effect	He^3 1530 MeV/c	H^3 1525 MeV/c	H^3 825 MeV/c
Multiple scattering of H^3 or He^3			
In target and dome	7.0	3.2	6.3
In counters	5.2	3.0	4.6
In He gas	3.0	1.7	2.4
Proton beam			
Angular divergence	3.1	3.1	1.6
Multiple scattering	1.9	1.9	1.0
Combined effects	9.9	6.0	8.3
Other factors			
	Full width at half-maximum (MeV/c)		
Effect	He^3 1530 MeV/c	H^3 1525 MeV/c	H^3 825 MeV/c
Finite angular definition and proton beam dimensions	7.5	10.1	9.7
Finite image and grid sizes	8.4	9.2	3.9
Combined effects	10.0	13.4	10.2
All effects (Full width at half-maximum)	26	19	22
Experimental	28	21	24

A. Factors Affecting the Momentum Resolution

1. Finite Angular Definition, Proton-Beam Dimensions, and Energy Loss in the Target

We treat these factors together since they are interdependent. The finite angular spread defined by the collimating slits affects the resolution in two ways. First, the momentum p is a kinematical function of the production angle θ of the H^3 or He^3. Second, the finite sensitive length of the target defined by the collimators requires that the produced particles have different path lengths R through the D_2 depending upon the position and angle at which they are produced. The finite width of the incident proton beam contributes in the same way. These factors are taken together, since there is a correlation between production angle and path length through the D_2. The amount of correlation in the momentum resolution depends upon the relative values of dp/dR and $dp/d\theta$.

2. Finite Image Size and Finite Grid Size

The finite dimensions of the sensitive region of the target were projected with approximately unit magnification (in runs 2 and 3) on the momentum-defining grids. This image was then folded in with the width of one grid to obtain an effective grid width.

3. Multiple Scattering of Momentum-Analyzed Beam

Materials that may multiply scatter the He^3 of H^3 with a subsequent loss of momentum resolution are the D_2 gas, the exit dome of the target, He bags, and the first counter in the time-of-flight path. Of these, scattering in the region of the target is the most important factor since it introduces a spread in production angle. Multiple scattering in S_1 (see Fig. 6 of paper I) makes the particles take a different angle through Q_2 and increases the effective grid width.

4. Angular Divergence of the Proton Beam

Angular divergence of the incoming proton beam increases the uncertainty in the production angle and contributes to the momentum resolution through $dp/d\theta$. The angular divergence may be roughly estimated from the dimensions of the premagnet collimator (Fig. 2 of paper I) and of the proton beam at the target position.

5. Multiple Scattering of the Proton Beam

This effect is small because the proton beam travels mainly in vacuum. The only important scattering materials are the 0.010-in. aluminum exit window of the vacuum tube, and the 0.005-in. Mylar and 0.019-in. stainless steel in the first half of the D_2 target.

6. Energy Spread of the Proton Beam

This factor is unknown and is determined by comparing our computed resolution functions with the experimental single-pion production peaks. The results indicate that a proton beam energy spread of about ± 2 MeV fits well. However there should be a tail extending farther on the low-energy side. This is consistent with that calculated from the beam geometry.

B. Results

The magnitudes of the effects contributing to the momentum resolution are shown in Table II for the three peaks observed in the second run. The computed resolution functions are compared with the experimental data in Figs. 1 (a), (b), and (c). In a similar way, the resolution at momenta corresponding to the $I=0$ anomaly was calculated. A comparison to the observed width of the anomaly is given in paper IV.

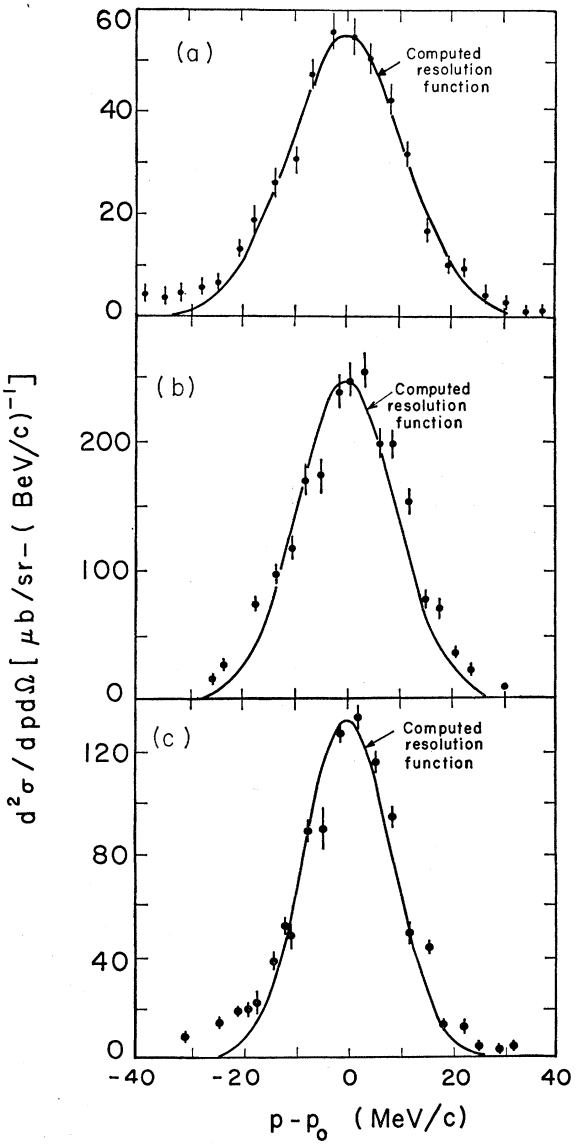

FIG. 1. Comparison of calculated resolution functions with measurements of the He^3 and H^3 momenta from the reactions $p+d\rightarrow He^3+\pi^0$ and $p+d\rightarrow H^3+\pi^+$ at a laboratory angle of 11.8 deg and an incident proton energy of 743 MeV. (a) He^3 peak at 1534 MeV/c, (b) H^3 peak at 824 MeV/c, and (c) H^3 peak at 1525 MeV/c.

IV. FORM FACTOR

In order to calculate cross sections for the reaction $p+d\rightarrow H^3+\pi^+$ one can use the impulse approximation.[5] This method has been used by Ruderman[6] and Bludman[7] to fit experimental data on $p+d\rightarrow H^3+\pi^+$ at 341 MeV.[8] In their calculations Ruderman and Bludman assume that the π^+ is produced in the elementary collision $p+p\rightarrow d+\pi^+$ and then use the overlap of the deuteron and triton wave functions to find out how often the extra neutron in the original deuteron sticks together with the deuteron in $p+p\rightarrow d+\pi^+$ to give a triton in the final state. The relationship between the cross sections is

$$\frac{d\sigma}{d\Omega}(pd\rightarrow t\pi^+)=\frac{1}{3}\left(\frac{1}{\bar{\beta}_{pd}}\frac{E_t}{E_\pi+E_t}\right)\left(\bar{\beta}_{pp}\frac{E_\pi+E_d}{E_d}\right)\times[f(\mathbf{\Delta})]^2\left[\frac{d\sigma}{d\Omega}(pp\rightarrow d\pi^+)\right], \quad (1)$$

where the $\bar{\beta}$'s and E's are, respectively, velocities and total energies in the center-of-mass system. The quantity $\mathbf{\Delta}$ is the momentum transfer to the struck deuteron when a meson of momentum $\mathbf{q}$ is produced by an incoming proton of momentum $\mathbf{k}$, $\mathbf{\Delta}=\frac{1}{2}\mathbf{k}-\frac{1}{3}\mathbf{q}$. $[f(\mathbf{\Delta})]^2$ is the probability of forming a final state triton and we call this the form factor. $f(\mathbf{\Delta})$ is given in terms of the deuteron and triton wave functions $\psi_d(\mathbf{x})$ and $\psi_t(\mathbf{z},\mathbf{x})$ by

$$f(\mathbf{\Delta})=\int\psi_d(\mathbf{x})\exp(i\mathbf{\Delta}\cdot\mathbf{x})\frac{\psi_t(\mathbf{x},0)}{\psi_d(0)}d\mathbf{x}, \quad (2)$$

where $\mathbf{x}$ is the n-p relative coordinate and $\mathbf{z}$ is the coordinate of the other neutron in the triton relative to the c.m. system of the p and n.

Simple wave functions can be used which fit experimental angular distributions fairly well.[7,9] However, as Akimov *et al.* point out,[9] the energy dependence is not well reproduced, particularly at higher energies where the experimental $p+d\rightarrow H^3+\pi^+$ cross sections are higher than what the impulse approximation predicts. We also have been unable to fit all experimental data on $p+d\rightarrow H^3+\pi^+$ with the same normalization and same set of wave functions. However, since the angular distribution at a given energy is well reproduced, we can use experimental data at the energy of our experiments to compute $[f(\mathbf{\Delta})]^2$. If the wave functions $\psi_d=(e^{-\beta r}-e^{-\gamma r})/r$ and $\psi_t=e^{-K/2(x_{12}+x_{13}+x_{23})}$ are inserted into the expression (2) for $f(\mathbf{\Delta})$, the result is

$$|f(\mathbf{\Delta})|^2\propto\{[\Delta^2+(K+\beta)^2]^{-1}-[\Delta^2+(K+\gamma)^2]^{-1}\}^2. \quad (3)$$

Commonly used values of the wave function parameters are $\beta=0.229$ F^{-1}, $\gamma=6\beta$ and $K=0.907$ F^{-1}. The results of fitting Eq. (3) (neglecting the second term) to the ratio

$$(d\sigma/d\Omega)(p+d\rightarrow H^3+\pi^+)/(d\sigma/d\Omega)(p+p\rightarrow d+\pi^+)$$

at incident energies for the H^3 reaction of 743 MeV and 591 MeV[4] are shown in Fig. 2. The best fit for $(K+\beta)$ is 1.65 $(\hbar/\mu c)^{-1}$ whereas the accepted value

[5] G. F. Chew and M. L. Goldberger, Phys. Rev. **77**, 470 (1950).
[6] M. A. Ruderman, Phys. Rev. **87**, 383 (1952).
[7] S. A. Bludman, Phys. Rev. **94**, 1722 (1954).
[8] W. J. Frank, K. C. Bandtel, R. Madey, and B. J. Moyer, Phys. Rev. **94**, 1716 (1954).
[9] Y. K. Akimov, O. V. Savchenko, and L. M. Soroko, Zh. Eksperim. i Teor. Fiz. **41**, 708 (1961) [translation: Soviet Phys.—JETP **14**, 512 (1962)].

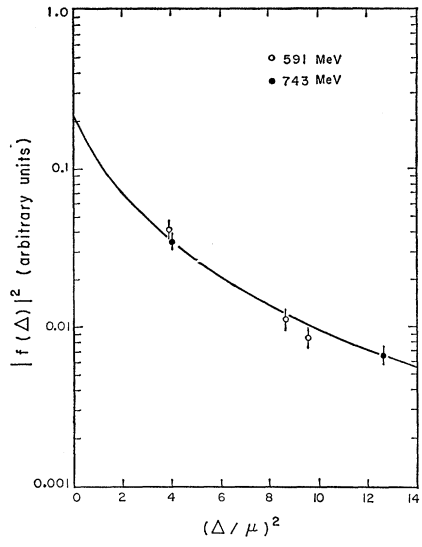

FIG. 2. Determination of the impulse-approximation form factor $|f(\mathbf{\Delta})|^2$ from experimental data on $p+d\rightarrow H^3+\pi^+$ at 591 and 743 MeV. The solid curve is the fit with $|f(\mathbf{\Delta})|^2\propto[(1.65)^2+\Delta^2]^{-2}$.

based on low-energy data is 1.605.[2] This agreement is good considering we have neglected γ and any hard core in the deuteron. We do not attempt to draw any conclusions about ψ_d and ψ_t from the experimental value of $(K+\beta)$, but consider it just a parameter in a theoretically-predicted form for $f(\mathbf{\Delta})$. We conclude that the single-pion production reactions $p+d\rightarrow He^3+\pi^0$ and $p+d\rightarrow H^3+\pi^+$ can be adequately expressed in terms of $(d\sigma/d\Omega)(p+p\rightarrow d+\pi^+)$ and $|f(\mathbf{\Delta})|^2$.

For the double-pion production reactions we should use the same $|f(\mathbf{\Delta})|^2$, but the angular distribution for $p+p\rightarrow d+2\pi$. This has been measured by B. Sechi Zorn[10] at $T_p=2.05$ BeV and is $(1+\cos^2\theta^*)$, where θ^* is the angle of the heavy particle in the c.m. system. This angular distribution is similar to that of $p+p\rightarrow d+\pi^+$ at 1.5 BeV, the energy which gives a pion of the same momentum in the c.m. system as $p+d\rightarrow H^3+\pi^+$ at 743 MeV. We can write:

$$(d\sigma/d\Omega)(p+d\rightarrow He^3+\pi^0)\propto|f(\mathbf{\Delta})|^2(1+\cos^2\theta^*) \quad (4)$$

and

$$(d^2\sigma/dpd\Omega)(p+d\rightarrow He^3+2\pi)\propto(\text{phase space})|f(\mathbf{\Delta})|^2(1+\cos^2\theta^*). \quad (5)$$

In terms of the laboratory momentum, $p_3=3\Delta$, we have

$$|f(\mathbf{\Delta})|^2\propto[1+(p_3/p_0)^2]^{-2} \quad \text{with} \quad p_0=693\ \text{MeV}/c.$$

[10] B. Sechi Zorn, Phys. Rev. Letters 8, 282 (1962), and (private communication).

In paper IV this information will be included in the analysis of the He^3 momentum spectra.

V. RATIO OF $1\pi/2\pi$ PRODUCTION IN $p+d$ COLLISIONS

A final point of observation is the apparently large amount of 2π production as compared to 1π at 740 MeV (see Fig. 12 of paper I). One might expect, in analogy with meson production in $\pi-N$ and N-N collisions, that 2π production would be only a few percent of 1π at this energy. Instead, we find the cross sections to be roughly comparable.

It is interesting to compare the $1\pi/2\pi$ ratio with the statistical model.[11] If ρ is the volume in phase space, then in the laboratory system we have

$$\left[\frac{d\rho}{d\Omega_3}(1\pi)\right]\Big/\left[\frac{d^2\rho}{dp_3d\Omega_3}(2\pi)\right]=\left\{\frac{p_3}{4[W_L-(p_1\omega_3/p_3)\cos\theta_3]}\right\}\Big/\left\{\frac{2\mu\Omega}{(2\pi)^3}\frac{\pi p_3^2}{2\omega_3}\left[\frac{(w^2/4\mu^2-1)}{w^2/\mu^2}\right]^{1/2}\right\}. \quad (6)$$

Here W_L is the laboratory energy of the $p+d$ system; p_1 is the momentum of the incident proton; θ_3, p_3, and ω_3 are respectively the laboratory angle, momentum, and total energy of He^3 or H^3; w is the total energy in the barycentric system of the two pions, and Ω is the Fermi volume.

Using the 1π H^3 and He^3 peaks at 1530 MeV/c and average points in the 2π continuum, we obtain for the radius r_0 in $\Omega=4/3(r_0/\mu)^3$, 1.65 and 2.9 pion Compton wavelengths for the H^3 and He^3 data, respectively. These rather large values for the radius, particularly in the He^3 case, perhaps may not mean too much. This result may indicate something about the mechanism of pion production and in a way may support our conclusion (see paper IV) of a strong attraction between the two pions in the $I=0$ state.

ACKNOWLEDGMENTS

The author wishes to thank Dr. G. F. Chew, Dr. K. M. Watson, and Dr. J. Gillespie for many helpful discussions. He is also grateful to the coauthors of paper I, Dr. A. Abashian, Dr. K. M. Crowe, Dr. E. H. Rogers, and R. E. Hill who collaborated in the measurements, for contributing to several aspects of this paper.

[11] E. Fermi, Progr. Theoret. Phys. (Kyoto) 5, 570 (1950).